Carbohydrate Polymers 94 (2013) 934–939

Contents lists available at SciVerse ScienceDirect

Carbohydrate Polymers

journal homepage: www.elsevier.com/locate/carbpol

# Preparation and enzymatic hydrolysis of nanoparticles made from single xyloglucan polysaccharide chain

Ilham Mkedder, Christophe Travelet, Amandine Durand-Terrasson, Sami Halila, Frédéric Dubreuil*, Redouane Borsali**

*Centre de Recherches sur les Macromolécules Végétales (CERMAV, CNRS UPR 5301), affiliated with the Université Joseph Fourier (UJF), member of the Institut de Chimie Moléculaire de Grenoble (ICMG) and member of the PolyNat Carnot Institute, 601 rue de la Chimie, BP 53, 38041 Grenoble cedex 9, France*

ARTICLE INFO

*Article history:*
Received 11 July 2012
Received in revised form 5 October 2012
Accepted 1 February 2013
Available online 10 February 2013

*Keywords:*
Xyloglucan
Endoglucanase
Enzymatic hydrolysis
Dynamic light scattering
Atomic force microscopy
Transmission electron microscopy

ABSTRACT

In this work, polysaccharide nanoparticles based on tamarind seeds xyloglucan are prepared, analyzed in term of characteristic sizes and morphology, and degraded by the action of a glycoside-hydrolase. Obtained in an aqueous $NaNO_2$ solution (0.1 M), these unaggregated nanoparticles have a characteristic diameter of ca. 60 nm (DLS, AFM and TEM measures). They are not compact, but highly swollen and look like hyperbranched and dendrimer-like (soft sphere model) structures. This observation is coherent with the native structure of the xyloglucan macromolecules which are themselves branched. The enzymatic hydrolysis by cellulase of *Trichoderma reesei* of the xyloglucan nanoparticles is investigated. In particular, the apparent mass molecular weight drastically decreases meaning that the xyloglucan nanoparticles are effectively fully hydrolyzed by the endo-β-(1,4)-glucanase. Furthermore, we observe that the enzyme has to uncoil the nanoparticles before cutting the $\beta$-(1→4) bonds and digesting the xyloglucan.



## 1. Introduction

Polysaccharides are abundant natural polymers and can come out of several resources: animal, algae, microorganisms or plants. They are an inexhaustible source of advanced and sustainable materials exhibiting usually non-toxicity, biodegradability, biocompatibility and sometimes biorecognition properties. In the field of the preparation of polysaccharide-based nanoparticles (Schatz & Lecommandoux, 2010; Sundar, Kundu, & Kundu, 2010), the drug delivery devices (Liu, Jiao, Wang, Zhou, & Ziyong, 2008) are particularly relevant and can be prepared by emulsification, desolvation or coacervation (Langer et al., 2003) depending on the desired targeted application.

Xyloglucan is a hemicellulose polysaccharide that is found in the primary cell wall of higher plants (Fry et al., 1993; Hayashi, 1989) and can be present in seeds like tamarind where it represents 50% (w/w) (Shankaracharya, 1998) of the storing energetic resources. The chemical structure of tamarind seed xyloglucan consists of a cellulose-like main chain of β-(1→4)-linked D-glucosyl residues that is regularly substituted at C-6 with α-D-xylosyl and α-D-galactosyl-(1→2)-α-D-xylosyl residues (Nishinari, Takemasa, Zhang, & Takahashi, 2007; York, Vanhalbeek, Darvill, & Albersheim, 1993). The availability of the xyloglucan (in term of quantity and purity) allowed the development of a large number of commercial, industrial and pharmacological applications (Gidley et al., 1991; Picout, Ross-Murphy, Errington, & Harding, 2003; Rao & Srivastava, 1973). It is widely used as thickeners, gelling agents or stabilizers in food industry in Japan and other Asian countries. Xyloglucan gels are used for drug delivery (Coviello, Matricardi, & Alhaique, 2006; Miyazaki et al., 1998), and recently xyloglucan-based nanoparticles were prepared to encapsulate an anti-cancer drug (Cao et al., 2010).

Nevertheless high molecular weight xyloglucan chains present some limitations such as uncontrolled water solubility and a high polydispersity which originate from their ability to form large aggregates via hydrogen bonding (Picout et al., 2003). Nevertheless, the partial degradation of the xyloglucan can be achieved by its digestion with endo-β-(1,4)-glucanase which cuts the backbone at unsubstituted D-glucose positions (Fanutti, Gidley, & Reid, 1993).

In the present paper, we prepared xyloglucan nanoparticles, which were characterized by dynamic light scattering (DLS), gel permeation chromatography (GPC), and transmission electron microscopy (TEM). In fact, DLS represents a powerful method for the characterization of biomacromolecules in solution and for monitoring their degradation (Lima, Soldi, & Borsali, 2009;

* Corresponding author at: Centre de Recherches sur les Macromolécules Végétales (CERMAV, CNRS UPR 5301), Affiliated with the Université Joseph Fourier (UJF), 601 rue de la Chimie, BP 53, 38041 Grenoble cedex 9, France. Tel.: +33 476037672.
** Corresponding author. Tel.: +33 476037640.
*E-mail addresses:* dubreuil@cermav.cnrs.fr (F. Dubreuil), borsali@cermav.cnrs.fr (R. Borsali).

0144-8617/$ – see front matter © 2013 Elsevier Ltd. All rights reserved.
http://dx.doi.org/10.1016/j.carbpol.2013.02.001

Wu, Zhou, & Wang, 1995) while AFM has been successfully used to image polysaccharides morphology or to probe the interaction forces with other biomacromolecules like polysaccharides or proteins (Liu, Fu, Zhu, Li, & Zhan, 2009; Lubambo et al., 2009; Murai, Hokonohara, Takagi, & Kawai, 2009). We then investigated the enzymatic hydrolysis of these nanoparticles by a commercial endo-β-(1,4)-glucanase from *Trichoderma reesei* using DLS and AFM as techniques of analysis. This study is mandatory for further use of xyloglucane based nanoparticles in drug delivery applications where it is important to know the response mechanism of the nanoparticle to a possible enzymatic hydrolysis.

## 2. Materials

Xyloglucan from *Tamarindus indicia* was supplied by Saiguru Food Gum Manufacturer Pvt. Ltd. (Mumbai, Maharashtra, India). The xyloglucan was dissolved in water, put to boil and filtered to remove insoluble compounds. Then it was lyophilized. The powder was stored before further use.

The apparent mass molecular weight of xyloglucan was determined to be $4 \times 10^5$ g/mol by gel permeation chromatography using a Waters GPCV Alliance 2000 chromatograph from Wyatt (USA) equipped with three online detectors (a differential refractometer, a viscometric detector and a light scattering detector MALLS) and a Shodex OHpak SB-805 HQ column (8–300 mm; exclusion limit, $4 \times 10^6$). The solution was injected at a concentration of $1 \times 10^{-3}$ g/L in 0.02% $NaN_3$ aqueous solution containing $NaNO_3$ (0.1 M) and EDTA (10 mM) as eluant and solvent.

Cellulase (C2730 from *T. reesei* ATCC 26921, ≥700 units/g) was purchased from Sigma and used without any purification.

## 3. Methods

### 3.1. Dynamic light scattering (DLS) of xyloglucan

#### 3.1.1. Sample preparation

Solutions for DLS measurement (1 g/L) were prepared with sodium nitrite $NaNO_2$ (0.1 M) made with ultrapure Milli-Q water. The solutions were stirred overnight, then heated at 80 °C for 2 h. To eliminate dust and other large particles, all samples were filtered through 0.45 and 0.22 μm cellulose acetate filter (Millipore) prior to measurements.

#### 3.1.2. DLS measurements

These measurements were performed using an ALV laser goniometer, which consists of a cylindrical 33 mW HeNe linear polarized laser with a 632.8 nm wavelength and an ALV-5000/EPP multiple-tau digital correlator with a 125 ns initial sampling time. The samples were kept at a constant temperature of 25 °C throughout the experiments. The accessible scattering angle of this equipment ranges from 40 up to 120°. All samples were systematically studied at 90°. The solutions were put in ordinary glass cells. The minimum sample volume required for an experiment was ca. 1 mL. The data acquisition was done with the ALV-correlator control software and the counting time for each sample was 300 s. The relaxation time distributions $A(q,t)$ were obtained using CONTIN analysis of the autocorrelation function $C(q,t)$.

### 3.2. Atomic force microscopy (AFM)

#### 3.2.1. Sample preparation

The substrate used in this work was hydrophilic silicon with an approximate dimension 1 cm × 1 cm. Perfectly cleaned silicon was obtained by chemical treatment of the substrate with piranha solution $H_2SO_4/H_2O_2$ mixture (70:30, v/v) at 80 °C for one hour, followed by intensive rinsing with water and dry blowing by $N_2$ (Fritzen-Garcia et al., 2009). 20 μL of the xyloglucan suspension (the same suspension as the one used for DLS measurements) was deposited on the hydrophilic silicon surface, and then dried overnight at room temperature in a dessicator.

#### 3.2.2. AFM imaging

AFM imaging was performed at room temperature using a Pico plus (Molecular Imaging, Phoenix, USA) commercial instrument using a 100 μm × 100 μm piezoelectric scanner. 512 × 512 data points were acquired. Images were obtained in tapping mode, using silicon tips with a spring constant of 48 N/m and a resonance frequency of approximately 190 kHz (VISTA probes). Data treatment (i.e. height measurements after baseline correction only) and presentation were realized with the help of Gwyddion software.

### 3.3. Transmission electron microscopy (TEM)

The morphology of the xyloglucan nanoparticles was examined using a Philips CM200 transmission electron microscope (FEI Company, Hillsboro, USA) operating at 120 kV. The images were recorded on Kodak SO163 films. Drops of the xyloglucan suspension (1 g/L) in nitrite sodium (0.1 M) were deposited onto glow discharged hydrophilic carbon-coated copper grids and negatively stained with 2% (w/v) uranyl acetate; the liquid in excess was blotted with filter paper.

### 3.4. Enzymatic hydrolysis

#### 3.4.1. Capillary viscometry

The hydrolytic action was monitored by measuring the changes in specific viscosity as a function of incubation time using an automatized capillary viscosimeter (Schott 531 10). The enzymatic degradation experiments were carried out at 25 °C with 15 mL aqueous solution of xyloglucan prepared in 0.1 M $NaNO_2$ (1 g/L). The commercial cellulase was diluted 10 times and 10 μL were added into the medium. The viscosity was measured every 5 min during hydrolysis and the specific viscosity was calculated as $(T - T_0)/T_0$ where $T_0$ is the flow time measured for the solvent and $T$ is the flow time of the reaction mixture containing the enzyme.

#### 3.4.2. Gel permeation chromatography (GPC)

The molar mass distributions for the intact and the enzymatically hydrolyzed xyloglucan samples were analyzed by SEC/MALS/RI. The intact xyloglucan and the hydrolysates were dissolved at a concentration of 1 g/L. All samples were filtered through a 0.22 μm cellulose acetate filter (Millipore) before the analysis. The data from the detectors were processed using ASTRA software (ASTRA V 5.3.4.14 from Technology Corp.). Refractive index increment dn/dc = 0.153 mL/g used for the calculations was determined using a refractometer Optilab rEX (Wyatt Technology). Double injections were made for all samples.

#### 3.4.3. Dynamic light scattering (DLS)

For enzymatic hydrolysis, 1 μL of cellulase from *T. reesei* (diluted 10 times in 0.1 M $NaNO_2$) was injected into 1 mL of xyloglucan suspension at a concentration of 1 g/L. The scattering intensity and the hydrodynamic radius were detected in real-time during the enzymatic hydrolysis. The reaction was followed for a period of 4 h.

#### 3.4.4. Atomic force microscopy (AFM)

For AFM experiments, xyloglucan nanoparticles dried onto silicon wafer were incubated with the cellulase for various periods of time at room temperature. The surface was then rinsed by water

and let dry overnight. AFM observation was carried out in tapping mode in air.

## 4. Results and discussion

### 4.1. Xyloglucan nanoparticles formation

Tamarind xyloglucan is water-soluble, but the individual macromolecules tend not to fully hydrate and consequently supramolecular aggregated species remain present, even in very dilute solutions. This is because the $\beta$-(1→4) cellulose-like backbone promotes interchain interactions, and thus the biopolymer exhibits a balance between hydrophobic and hydrophilic regions (Picout et al., 2003).

Dynamic light scattering technique has become a powerful tool used for the study of polysaccharides, and to follow the changes in the system when certain parameters are modified like polymer or salt concentration, pH variations, temperature and solvent (Röder, Morgenstern, Schelosky, & Glatter, 2001). Xyloglucan solutions have been prepared with various conditions in term of solvent (water, DMSO, DMAc/LiCl and $NaNO_2$), concentrations (from 0.01 to 10 g/L) and heating temperature (Freitas et al. (2005) observed that heating substantially reduced molecular aggregation in xyloglucan solutions). We observed that no uncontrolled aggregation occurs in the case of aqueous $NaNO_2$ solution (0.1 M), so it was chosen as the best solvent for our experiments (Kai, De Oliveira, & Petkowicz, 2010). As $NaNO_2$ is known to oxidize polysaccharides on C-3 position in presence of phosphoric acid (Arendt, Carrière, Bouchez, & Sachetto, 1973; Hoffman, Larm, Lartsson, & Scholander, 1985) we controlled via NMR and IR spectroscopy that we did not damage our polymer. The autocorrelation function $C(q,t)$ and the distribution of the relaxation times $A(q,t)$ at a scattering angle of 90° for the suspension prepared in $NaNO_2$ (0.1 M) at a xyloglucan concentration of 1 g/L are reported in Fig. 1A. The apparent hydrodynamic radius at 90° of xyloglucan was $R_{h\,90°}$ = 28.0 nm. The two small peaks which appear at the lowest relaxation times cannot correspond to particles. Indeed, the obtained characteristic sizes would be smaller than the carbon–carbon bond length. Anyhow, they can be reasonably attributed to internal modes or to artifacts. The straight proportional behavior of the relaxation frequency ($1/\tau$) on the square of the modulus of the wave vector ($q^2$) proves the Brownian diffusive motion of the xyloglucan nanoparticles (Fig. 1B). From the slope (i.e. the nanoparticle diffusion coefficient) of this curve, *the* hydrodynamic radius was determined using the Stokes-Einstein relation (Mazzarino et al., 2012) and was found to be $R_h$ = 32.7 nm. The apparent hydrodynamic radius at a given observation angle should not be confused with the hydrodynamic radius obtained from the angular dependency. Both values are close one to the other in the case of monodisperse nanoparticles what is presently not the case.

Ultraviolet–visible spectroscopy shows that the xyloglucan nanoparticles suspension does not absorb at the wavelength used in the light scattering experiments, i.e. λ = 632.8 nm (data not shown).

Furthermore gel permeation chromatography analysis shows that xyloglucan has the apparent mass molecular weight $M_{w\,app} = 1.8 \times 10^5$ g/mol (pullulans having different molecular weights are used as standards). This value is slightly lower than that obtained by Muller et al. (2011) ($4.6 \times 10^5$ g/mol). We obtained the radius of gyration $R_g$ = 32.0 nm and the hydrodynamic radius $R_h$ = 24.0 nm. This latter value is relatively close to the one obtained using the classical dynamic light scattering device (i.e. $R_h$ = 32.7 nm).

The experimental $\rho$-parameter is known to give a more precise idea on the morphology of the present nanoparticles. Experimentally we get $\rho = R_g/R_h = 1.3$ when using the gel permeation chromatography results and 1.0 when combining dynamic light scattering and gel permeation chromatography results. These values correspond to hyperbranched and dendrimer-like (soft sphere model) structures (Burchard, 2005) implying the presence of highly swollen nanoparticles, and are coherent with the native structure of the xyloglucan macromolecules that are themselves branched. Furthermore, based on those observations we can establish that we got single chains nanoparticles and that using sodium nitrite during solubilization (with concentrations ranging from 0.1 to 1 M) reduces the inter chains hydrogen bonds responsible of the classical aggregation of the polysaccharides.

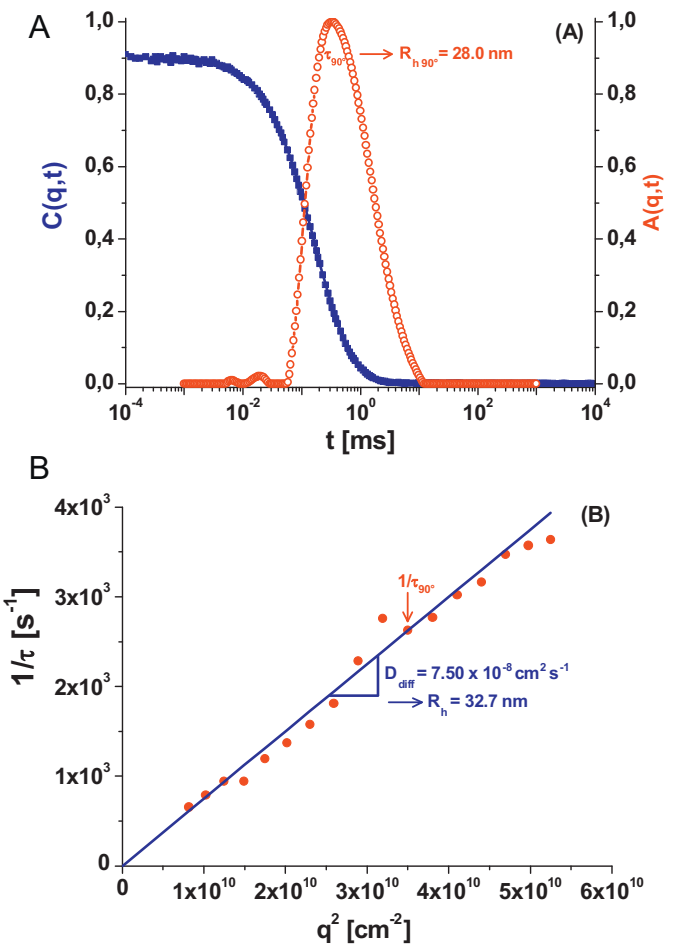


**Fig. 1.** DLS: (A) autocorrelation function $C(q,t)$ and distribution of the relaxation times $A(q,t)$ at a scattering angle of 90° for the xyloglucan suspension prepared in $NaNO_2$ (0.1 M) at 1 g/L. (B) Dependence of the relaxation frequency ($1/\tau$) on the square of the modulus of the wave vector ($q^2$) between 40 and 120° by step of 5°.

Static light scattering technique cannot be used to go deeper in the morphology study of the xyloglucan nanoparticles. Indeed they are too small. Thus atomic force microscopy and transmission electron microscopy were chosen.

The dried sample was visualized by atomic force microscopy in tapping mode in an area of 3 μm × 3 μm as shown in Fig. 2A. Xyloglucan nanoparticles with a height of ca. 40 nm are observed in the topography image. This value is notably smaller than $2R_h$ = 65.4 nm and $2R_g$ = 64.0 nm obtained here above by dynamic light scattering and gel permeation chromatography respectively. This apparent contradiction is explained by the fact that the highly swollen nanoparticles are floppy due to their hyperbranched and dendrimer-like (soft sphere model) nature, and become thus quite flat upon drying. The lateral size of the nanoparticles is drastically increased by the tip shape (tip radius of ca. 20 nm) and the deformation of the nanoparticles upon drying. They well adhered to

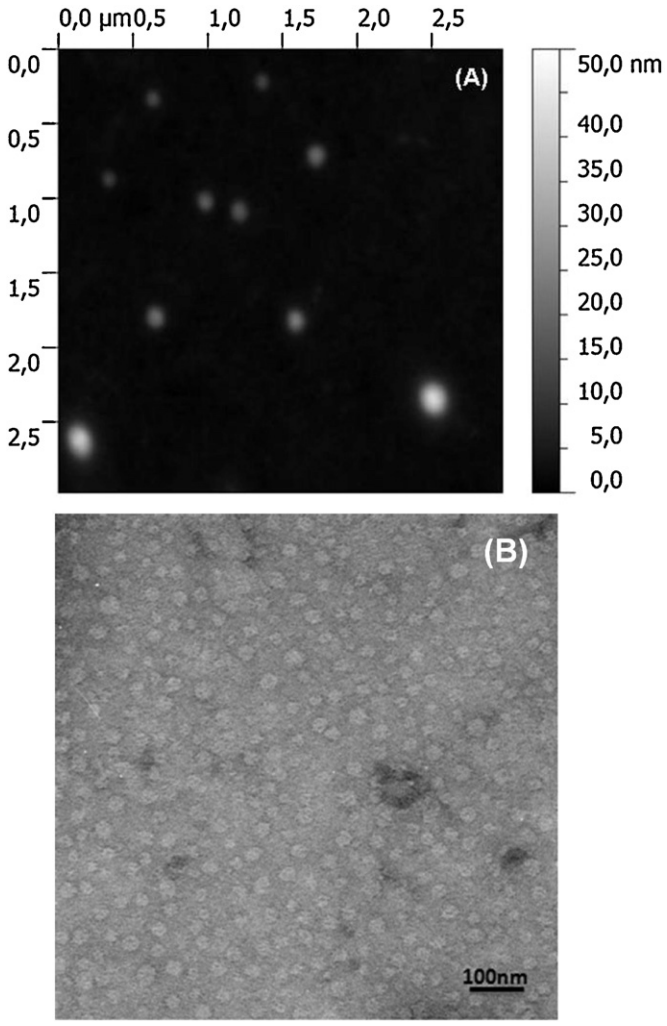


**Fig. 2.** (A) AFM topography image (3 µm × 3 µm) obtained from xyloglucan nanoparticles deposited on hydrophilic silicon substrate. (B) TEM image obtained from xyloglucan nanoparticles deposited on glow discharged hydrophilic carbon-coated copper grids and negatively stained with 2% (w/v) uranyl acetate.

the surface and were not quantitatively removed by rinsing due to favorable particle-substrate affinity. From transmission electron microscopy (Fig. 2B), it is noted that xyloglucan form unaggregated nanoparticles whose characteristic diameter is ca. 56 nm (mean value obtained over 134 nanoparticles). The nanoparticles appear here also relatively flat. Anyhow their apparent diameter is compatible with the values $2R_h$ = 65.4 nm and $2R_g$ = 64.0 nm obtained here above by dynamic light scattering and gel permeation chromatography respectively (i.e. in presence of solvent) due to a compensation between the nanoparticle flattening upon drying and the nanoparticle retraction coming from the uranyl acetate.

The results obtained using 4 complementary characterization methods are coherent. Some differences in the sizes were attributed to the drying. However we obtained stable unaggregated nanoparticles consisting of a single polysaccharide chain.

### 4.2. Xyloglucan nanoparticle enzymatic hydrolysis

The aim of this work is to investigate the enzymatic hydrolysis by cellulase from *T. reesei* of the xyloglucan nanoparticles described here above using different methods of analysis in solution or at a solid interface. *T. reesei* is a filamentous fungus which secretes exceptional amounts of cellulolytic enzymes, cellobiohydrolase or *exo*cellulase, and *endo*glucanase.

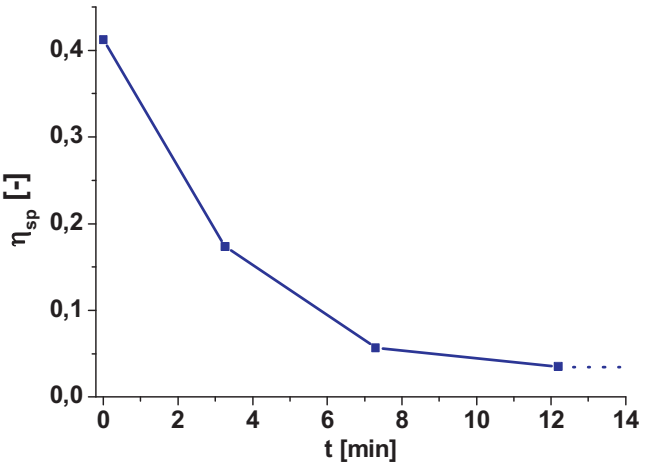


**Fig. 3.** Capillary viscosimetry: dependence of the specific viscosity ($\eta_{sp}$) on the incubation time ($t$) for the xyloglucan suspension prepared in $NaNO_2$ (0.1 M) at 1 g/L incubated with endo-β-(1,4)-glucanase.

The hydrolytic activity of β-1-4-endoglucanase was analyzed with capillary viscosimetry studying the decrease in specific viscosity of the xyloglucan suspension as function of incubation time. The specific viscosity decreases rapidly by a factor 11.7 with a characteristic time of ca. 4.5 min (Fig. 3). After 12 min no change is observed anymore and the specific viscosity of the solvent is measured.

Molar mass determination of the intact and enzymatically hydrolyzed xyloglucans was performed using gel permeation chromatography in order to investigate the extent of the hydrolysis (Table 1). Not only the apparent mass molecular weight but also the radius of gyration and the hydrodynamic radius drastically decrease meaning that the xyloglucan nanoparticles were effectively hydrolyzed by the endoglucanase. The apparent mass molecular weight of the final degradation product reaches ca. 4000 g/mol which corresponds to two xyloglucan residues and thus to a full degradation.

Light scattering allows in real time the observation of the hydrolysis. Therefore we studied the time dependence of the light scattering intensity (Fig. 4). We know that the scattering intensity is proportional to both the concentration and the apparent mass molecular weight. During the first 30 min of enzymatic hydrolysis the scattering intensity decreased sharply which a characteristic time of ca. 25 min. This characteristic value is higher than that obtained in the case of viscosity measurements. After 100 min we reach a plateau indicating the end of the reaction. During this process we also followed the intensity fluctuations at 90° to get the hydrodynamic radius ($R_h$) of the nanoparticles (Table 2). Prior to the hydrolysis the $R_h$ of the enzyme was estimated by dynamic light scattering to be 4 nm. We notice a decrease of the nanoparticle size from 28 down to 18 nm during the first 20 min, and then an increase from 18 up to 43 nm. This latter value remains stable from 100 to 300 min.

During the enzymatic hydrolysis, β-1-4-endoglucanase break the β-1-4 links in the main chain of xyloglucan at unsubstituted glucosidic residues (Scheme 1), and oligo-xyloglucans are formed

**Table 1**
GPC results for the intact xyloglucan nanoparticles prepared in $NaNO_2$ (0.1 M) at 1 g/L ($XG_1$), and the enzymatically hydrolyzed xyloglucan nanoparticles prepared in $NaNO_2$ (0.1 M) at 1 g/L incubated with endo-β-(1,4)-glucanase ($XG_2$) (apparent mass molecular weight $M_{w\,app}$, radius of gyration $R_g$ and hydrodynamic radius $R_h$).

| Sample | $M_{w\,app}$ (g/mol) | $R_g$ (nm) | $R_h$ (nm) |
|---|---|---|---|
| $XG_1$ | 180 000 | 32.2 | 24.5 |
| $XG_2$ | 4 140 | 12.2 | 1.6 |

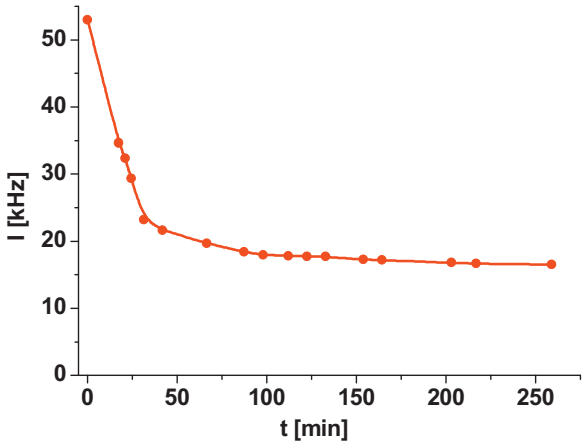


**Fig. 4.** Light scattering: dependence of the scattering intensity ($I$) on the incubation time ($t$) at a scattering angle of 90° for the xyloglucan suspension prepared in $NaNO_2$ (0.1 M) at 1 g/L incubated with β-1-4-endoglucanase.

**Table 2**
DLS: dependence of the apparent hydrodynamic radius at 90° ($R_{h\,90°}$) on the incubation time ($t$) for the xyloglucan suspension prepared in $NaNO_2$ (0.1 M) at 1 g/L incubated with β-1-4-endoglucanase.

| $t$ (min) | $R_{h\,90°}$ (nm) |
|---|---|
| 0 | 28 |
| 20 | 18 |
| 30 | 26 |
| 60 | 32 |
| 90 | 41 |
| 200 | 43 |

implying a decrease of the scattering intensity and of the $R_h$. The oligo-xyloglucans then combine in order to form few aggregates. It implies an increase of $R_h$ whereas the scattering intensity remains constant. At the end of the reaction, the characteristic peak of the enzyme at 4 nm is found again and proves the enzymatic character of the reaction.

The cellulase was used to hydrolyze the xyloglucan nanoparticles adsorbed on a silicon wafer. The hydrolysis and the atomic force microscopy experiments were performed after the xyloglucan nanoparticles are adsorbed and dried onto a silicon wafer. Fig. 5 shows two representative topography pictures obtained after the treatment of the xyloglucan nanoparticles with β-1-4-endoglucanase for various time intervals (30 min and 4 h). These images must be compared with Fig. 2A which was obtained before the addition of the enzyme, and can thus be defined as the zero time point. This previous image reflects clearly the xyloglucan presence under the shape of nanoparticles only. After incubation of the xyloglucan nanoparticles with the enzyme for 30 min, chains are visible in the image (Fig. 5A), and a few nanoparticles with a

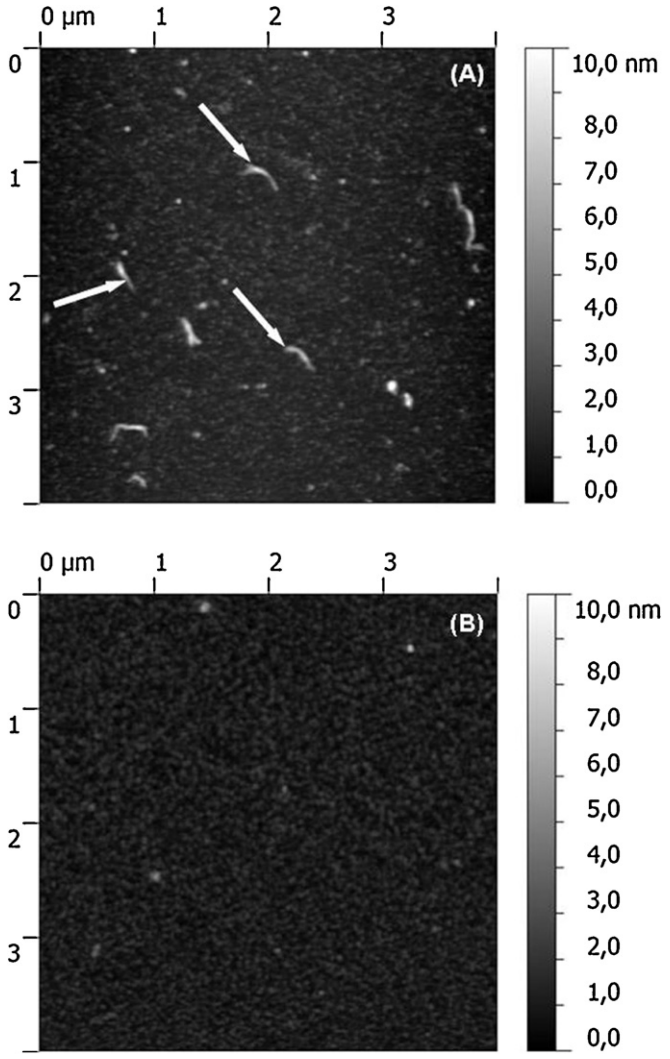


**Fig. 5.** AFM topography images (4 µm × 4 µm) obtained from the xyloglucan suspension prepared in $NaNO_2$ (0.1 M) at 1 g/L deposited on hydrophilic silicon substrate and incubated with β-1-4-endoglucanase (A) for 30 min, and (B) for 4 h.

diameter from 5 to 12 nm are present. The final image (Fig. 5B) obtained after 4 h incubation shows that after such a long time no xyloglucan nanoparticle can be found, despite extensive searching of the surface. This confirms that the enzyme can carry on an activity on the xyloglucan nanoparticles adsorbed on a surface. On the other hand, the strong adhesion of xyloglucan nanoparticles onto a silicon wafer was established. The images also demonstrate that atomic force microscopy can be used to follow the mechanism of enzymatic hydrolysis of polysaccharides. In addition, the action

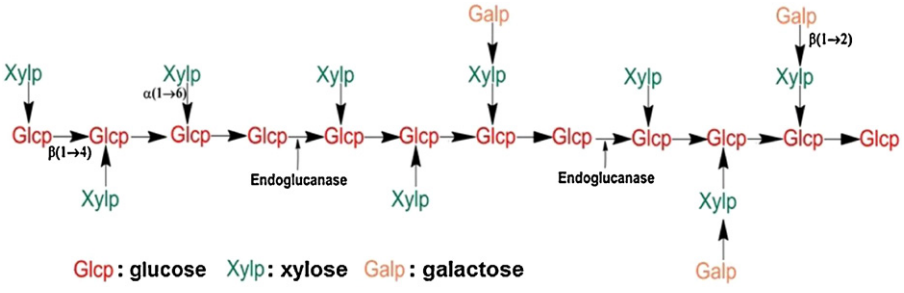


**Scheme 1.** Schematic representation of the hydrolysis of xyloglucan by endoglucanase.

mechanism of the cellulase on the xyloglucan nanoparticles can be guessed: Before cutting the $\beta$-(1→4) bonds, the enzyme has to uncoil the nanoparticles (Fig. 5A). The image also reveals that the duration of degradation is slower than that obtained by light scattering. We think it is due to a surface effect.

## 5. Conclusion

In this study, we demonstrated that it is possible to obtain single chain nanoparticles based on xyloglucan using a simple preparation method (a specific solvent) without the help of any cross linking agent or complex co-precipitation method.

Those nanoparticles have been fully characterized by DLS, AFM and TEM. We also deduced that those nanoparticles are not compact, but highly swollen like hyperbranched structures.

Monitoring the enzymatic hydrolysis of these nanoparticles by dynamic light scattering indicated the aggregation of the degradation products. Using AFM, it was shown that the enzyme is able to degrade the nanoparticles adsorbed on a surface and a possible action mechanism of the enzyme has been established.

Further studies combining DLS and in situ AFM would be of great interest for the development of new polysaccharide based nanoparticles for potential applications.

## Acknowledgments

The authors thank NanoBio platform in Grenoble for granting access to AFM facilities. IM thanks the Algerian Government for financial support during PhD period.

## References

Arendt, J. H., Carrière, J. P., Bouchez, P., & Sachetto, J. P. (1973). Oxidation of cellulose by acid-sodium nitrite systems. *Journal of Polymer Science: Polymer Symposia*, *42*, 1521–1529.

Burchard, W. (2005). *Polysaccharides: Structural diversity and functional versatility*. New York: Dekker.

Cao, Y., Gu, Y., Ma, H., Bai, J., Liu, L., Zhao, P., et al. (2010). Self-assembled nanoparticle drug delivery systems from galactosylated polysaccharide-doxorubicin conjugate loaded doxorubicin. *International Journal of Biological Macromolecules*, *46*, 245–249.

Coviello, T., Matricardi, P., & Alhaique, F. (2006). Drug delivery strategies using polysaccharidic gels. *Expert Opinion on Drug Delivery*, *3*, 395–404.

Fanutti, C., Gidley, M. J., & Reid, J. S. G. (1993). Action of a pure xyloglucan endo-transglycosylase (formerly called xyloglucan-specific endo-(1→4)-β-D-glucanase) from the cotyledons of germinated nasturtium seeds. *Plant Journal*, *3*, 691–700.

Freitas, R. A., Martin, S., Santos, G. L., Valenga, F., Buckeridge, M. S., Reicher, F., et al. (2005). Physico-chemical properties of seed xyloglucans from different sources. *Carbohydrate Polymers*, *60*, 507–514.

Fritzen-Garcia, M. B., Zanetti-Ramos, B. G., De Oliveira, C. S., Soldi, V., Pasa, A. A., & Creczynski-Pasa, T. B. (2009). Atomic force microscopy imaging of polyurethane nanoparticles onto different solid substrates. *Materials Science and Engineering C*, *29*, 405–409.

Fry, S. C., York, W. S., Albersheim, P., Darvill, A., Hayashi, T., Joseleau, J.-P., et al. (1993). An unambiguous nomenclature for xyloglucan-derived oligosaccharides. *Physiologia Plantarum*, *89*, 1–3.

Gidley, M. J., Lillford, P. J., Rowlands, D. W., Lang, P., Dentini, M., Crescenzi, V., et al. (1991). Structure and solution properties of tamarind-seed polysaccharide. *Carbohydrate Research*, *214*, 299–314.

Hayashi, T. (1989). Xyloglucans in the primary cell wall. *Annual Review of Plant Physiology and Plant Molecular Biology*, *40*, 139–168.

Hoffman, J., Larm, O., Lartsson, K., & Scholander, E. (1985). Oxidation of dextran NRRL B-512 with sodium nitrite in phosphoric acid. *Acta Chemica Scandinavica. Series B. Organic Chemistry and Biochemistry*, *39*, 513–515.

Kai, K. C., De Oliveira, C. L., & Petkowicz, C. L. (2010). Influence of extraction conditions on properties of seed xyloglucan. *International Journal of Biological Macromolecules*, *46*, 223–228.

Langer, K., Balthasar, S., Vogel, V., Dinauer, N., von Briesen, H., & Schubert, D. (2003). Optimization of the preparation process for human serum albumin (HSA) nanoparticles. *International Journal of Pharmaceutics*, *257*, 169–180.

Lima, A. M. F., Soldi, V., & Borsali, R. (2009). Dynamic light scattering and viscosimetry of aqueous solutions of pectin, sodium alginate and their mixtures: Effects of added salt, concentration, counterions, temperature and chelating agent. *Journal of the Brazilian Chemical Society*, *20*, 1705–1714.

Liu, H., Fu, S., Zhu, J., Li, H., & Zhan, H. (2009). Visualization of enzymatic hydrolysis of cellulose using AFM phase imaging. *Enzyme and Microbial Technology*, *45*, 274–281.

Liu, Z., Jiao, Y., Wang, Y., Zhou, C., & Zhang, Z. (2008). Polysaccharides-based nanoparticles as drug delivery systems. *Advanced Drug Delivery Reviews*, *60*, 1650–1662.

Lubambo, A. F., Lucyszyn, N., Klein, J. J., Schreiner, W. H., De Camargo, P. C., & Sierakowski, M. R. (2009). Dewetting pattern and stability of thin xyloglucan films adsorbed on silicon and mica. *Colloids and Surfaces B: Biointerfaces*, *70*, 174–180.

Mazzarino, L., Travelet, C., Ortega-Murillo, S., Otsuka, I., Pignot-Paintrand, I., Lemos-Senna, E., et al. (2012). Elaboration of chitosan-coated nanoparticles loaded with curcumin for mucoadhesive applications. *Journal of Colloid and Interface Science*, *370*, 58–66.

Miyazaki, S., Suisha, F., Kawasaki, N., Shirakawa, M., Yamatoya, K., & Attwood, D. (1998). Thermally reversible xyloglucan gels as vehicles for rectal drug delivery. *Journal of Controlled Release*, *56*, 75–83.

Muller, F., Manet, S., Jean, B., Chambat, G., Boué, F., Heux, L., et al. (2011). SANS measurements of semiflexible xyloglucan polysaccharide chains in water reveal their self-avoiding statistics. *Biomacromolecules*, *12*, 3330–3336.

Murai, T., Hokonohara, H., Takagi, A., & Kawai, T. (2009). Atomic force microscopy imaging of supramolecular organization of hyaluronan and its receptor CD44. *IEEE Transactions on NanoBioscience*, *8*, 294–299.

Nishinari, K., Takemasa, M., Zhang, H., & Takahashi, R. (2007). Storage plant polysaccharides: Xyloglucans, galactomannans, glucomannans. *Comprehensive Glycoscience*, *2*, 613–652.

Picout, D. R., Ross-Murphy, S., Errington, N., & Harding, S. E. (2003). Pressure cell assisted solubilization of xyloglucans: Tamarind seed polysaccharide and detarium gum. *Biomacromolecules*, *24*, 799–807.

Rao, P. S., & Srivastava, H. C. (1973). *Industrial gums: Polysaccharides and their derivatives*. New York: Academic Press. (chapter 17: Tamarind).

Röder, T., Morgenstern, B., Schelosky, N., & Glatter, O. (2001). Solutions of cellulose in N,N-dimethylacetamide/lithium chloride studied by light scattering methods. *Polymer*, *42*, 6765–6773.

Schatz, C., & Lecommandoux, S. (2010). Polysaccharide-containing block copolymers: Synthesis, properties and applications of an emerging family of glycoconjugates. *Macromolecular Rapid Communications*, *31*, 1664–1684.

Shankaracharya, N. B. (1998). Tamarind – Chemistry, technology and uses – A critical appraisal. *Journal of Food Science and Technology*, *35*, 193–208.

Sundar, S., Kundu, J., & Kundu, S. C. (2010). Biopolymeric nanoparticles. *Science and Technology of Advanced Materials*, *11*, 1468–1480.

Wu, C., Zhou, S., & Wang, W. (1995). A dynamic laser light-scattering study of chitosan in aqueous solution. *Biopolymers*, *35*, 385–392.

York, W. S., van Halbeek, H., Darvill, A. G., & Albersheim, P. (1993). Structural analysis of xyloglucan oligosaccharides by 1H-n.m.r. spectroscopy and fast-atom-bombardment mass spectrometry. *Carbohydrate Research*, *200*, 9–31.